

Direct Arylations for Study of the Air-Stable P-Heterocyclic Biradical: From Wide Electronic Tuning to Characterization of the Localized Radicalic Electrons

Shigekazu Ito,^{*,†} Yasuhiro Ueta,[†] Trang Thi Thu Ngo,[†] Makoto Kobayashi,[†] Daisuke Hashizume,[‡] Jun-ichi Nishida,[§] Yoshiro Yamashita,[§] and Koichi Mikami[†]

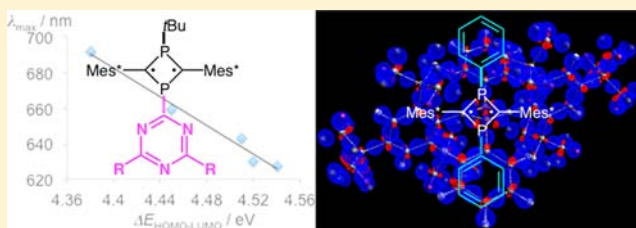
[†]Department of Applied Chemistry, Graduate School of Science and Engineering, Tokyo Institute of Technology, 2-12-1 Ookayama, Meguro, Tokyo 152-8552, Japan

[‡]Materials Characterization Support Unit, RIKEN Center for Emergent Matter Science, 2-1 Hirosawa, Wako, Saitama 351-0198, Japan

[§]Department of Electronic Chemistry, Interdisciplinary Graduate School of Science and Engineering, Tokyo Institute of Technology, 4259 Nagatsuta, Midori-ku, Yokohama 226-8502, Japan

Supporting Information

ABSTRACT: We have developed methods for installing aryl substituents directly on the phosphino groups of the 1,3-diphosphacyclobutane-2,4-diyl system. The aryl substituents tuned the electronic and structural characteristics of the biradical unit both in solution and in the solid state. 1-*tert*-butyl-2,4-bis(2,4,6-tri-*tert*-butylphenyl)-1,3-diphosphacyclobutene-4-yl anion, prepared from phosphalkyne ($\text{Mes}^*\text{C}\equiv\text{P}$; $\text{Mes}^* = 2,4,6\text{-}t\text{Bu}_3\text{C}_6\text{H}_2$) and *t*-butyllithium, was allowed to react with an electron-deficient N-heterocyclic reagent. The corresponding N-heteroaryl-substituted P-heterocyclic biradicals were produced via $\text{S}_{\text{N}}\text{Ar}$ reactions. Biradicals bearing perfluorinated pyridyl substituents exhibited photoabsorption properties comparable to those of previously reported derivatives because the highest occupied and lowest unoccupied molecular orbital levels were reduced by a similar amount. In contrast, the triazine substituent reduced the band gap of the biradical unit, and the large red shift in the visible absorption and high oxidation potential were further tuned via subsequent $\text{S}_{\text{N}}\text{Ar}$ and Negishi coupling reactions. The amino-substituted triazine structure provided a strongly electron-donating biradical chromophore, which produced unique p-type semiconducting behavior even though there was no obvious π -overlap in the crystalline state. The single-electron transfer reaction involving $\text{Mes}^*\text{C}\equiv\text{P}$, phenyllithium, and iodine afforded 1,3-diphenyl-2,4-bis(2,4,6-tri-*tert*-butylphenyl)-1,3-diphosphacyclobutane-2,4-diyl via the intermediate P-heterocyclic monoradical. The tetraaryl-substituted symmetric biradical product was used to determine the electron density distribution from the X-ray diffraction data. The data show highly localized radicalic electrons around the skeletal carbon atoms, moderately polarized skeletal P–C bonds in the four-membered ring, and no covalent transannular interaction.



INTRODUCTION

Highly stabilized reaction intermediates such as radicals¹ have been important in furthering molecular science and in developing various functional materials for electronics and biology. Biradicals, which bear two radical centers, are usually too unstable to isolate under ordinary conditions. For example, an observable cyclobutane-1,3-diyl under cryogenic conditions is promptly converted to the corresponding bicyclo[1.1.0]butane upon heating.^{2,3} However, Niecke and co-workers isolated the first room temperature stable 1,3-diphosphacyclobutane-2,4-diyl **A** ($\text{Mes}^* = 2,4,6\text{-}t\text{Bu}_3\text{C}_6\text{H}_2$), which is a congener of cyclobutanediyl, by using sterically encumbered 2,2-dichloro-1-phosphaethene (Figure 1, left).^{4,5} The isolation of **A** confirmed that the electronic effects of the heavier main group elements^{6–8} can be exploited to produce stable biradicals.

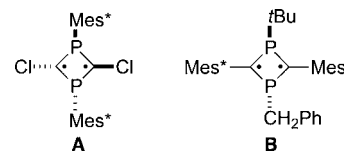


Figure 1. Isolable 1,3-diphosphacyclobutane-2,4-diyls.

Although **A** exhibits considerable thermal stability, it is highly air- and moisture-sensitive, probably because of insufficient steric protection around the radicalic carbon centers. Subsequent studies of P-heterocyclic biradicals suggested that bulky Mes^* groups adjacent to the radical centers stabilize the biradical skeleton effectively (Figure 1, right). We used

Received: September 20, 2013

Published: October 16, 2013

phosphaalkyne chemistry to synthesize air-tolerant crystalline 1,3-diphosphacyclobutane-2,4-diyl **B**, and the high stability of **B** was valuable for investigating functional materials based on the biradical moiety.^{9–11} Very recently, we reported the scope of the through-space electrostatic interaction between the electron-donating biradical chromophores, which would be useful for developing functional materials based on mixed-valent structures.¹²

Understanding the conjugative interaction between the P-heterocyclic moiety and π -electron systems is important for developing the chemistry of stable biradicals. We expect that the conjugative interaction between the P-aryl moiety and the cyclic biradical unit will be unusual and useful for wider applications.¹³ However, tuning the biradical unit with direct P–aryl bonding has not been investigated extensively. Niecke and co-workers used the Mes*P moiety as the reactive functional group, which provided the monoradical upon irradiation^{5d} and the dianion upon alkaline reduction.^{5e} Direct P–aryl bonding to the biradical system has not been thoroughly investigated because of the lack of synthetic methods.

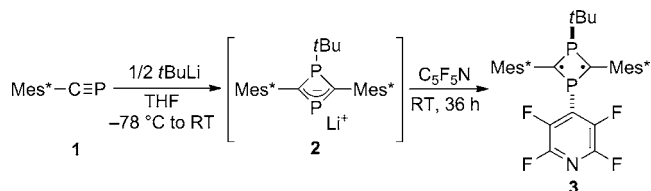
Furthermore, although the number of isolable congeners of cyclobutanediyl has increased, the stable biradical structure is still debated on the basis of the contribution of the resonance structures^{4,8,14} and the effect of the possible transannular interaction.¹⁵ Even though a number of stable cyclic biradical derivatives have been reported, their structures have not been investigated well. Therefore, the structural characteristics of the P-heterocyclic biradical skeleton have yet to be determined. Very recently, Stalke and co-workers succeeded in experimental charge density determination of an isomer of hexasilabenzene, which is topologically related to 1,3-diphosphacyclobutane-2,4-diyl.¹⁶

In this study, we demonstrate that electron-deficient N-heteroaryl groups can be installed directly on the P-heterocyclic biradical skeleton via a nucleophilic aromatic substitution (S_NAr) reaction. The N-heteroaryl groups altered the physicochemical properties and crystalline structure of the biradicals. Furthermore, we discuss the p-type semiconducting properties induced by the strongly electron-donating amino-substituted *s*-triazine group with the properties of **B**. We obtained X-ray diffraction data from single crystals of the symmetrical tetraaryl-substituted 1,3-diphosphacyclobutane-2,4-diyl, synthesized by a single-electron transfer (SET) reaction, which showed the radicalic electrons localized around the skeletal carbons as well as the polarized P–C bonds and no transannular bonding.

RESULTS AND DISCUSSION

S_NAr Reaction for Pyridyl-Substituted 1,3-Diphosphacyclobutane-2,4-diyls. Phosphaalkyne **1** was treated with 0.5 equiv of *tert*-butyllithium in THF to generate the corresponding cyclic anion **2**, and the room temperature stable THF solution of **2** was allowed to react with perfluoropyridine (Scheme 1).¹⁷ After the reaction mixture was stirred for 36 h, the S_NAr reaction was terminated, and the perfluoropyridyl-substituted 1,3-diphosphacyclobutane-2,4-diyl **3** was obtained as a deep-blue crystalline compound in 43% yield. Crystalline compound **3** showed high stability in air over at least 6 months, probably because of the steric and electronic effects of the fluorinated N-heteroaryl structure. We expected that the perfluorination of pyridine would be a suitable S_NAr reaction for constructing the direct phosphorus–perfluoroaryl linkage through the facile

Scheme 1. S_NAr Reaction of **2** with Perfluoropyridine



elimination of fluoride. In fact, **2** can also behave as a leaving group,^{11b,18} and the attempted synthesis of similar aryl-substituted 1,3-diphosphacyclobutane-2,4-diyls with hexafluorobenzene, pentafluorobenzene, pentafluoriodobenzene, 1-fluoro-2,4-dinitrobenzene, 2-chloropyridine, 2-chloro-5-(trifluoromethyl)pyridine, 2-chloro-5-(trifluoromethyl)pyridine *N*-oxide, and 3,5-dichloro-2,4,6-trifluoropyridine as electrophiles failed. Reactions of **2** with pentafluorobenzonitrile and octafluorotoluene gave small amounts of the corresponding products together with nonseparable byproducts (see the Supporting Information).

We expected the fluorine atoms in **3** to be available for further substitution reactions.^{17c} However, the presence of the electron-rich P-heterocyclic system prevented the expected S_NAr reactions of **3** with 2-pyridyllithium, [4-(trifluoromethyl)phenyl]lithium, lithium 2-phenylacetylide, sodium *tert*-butoxide, diethylamine, and butyllithium. The S_NAr reaction of two fluorine atoms in **3** took place when **3** was treated with more than 2 equiv of phenyllithium, and the corresponding product **4** was obtained in 71% isolated yield (Scheme 2). Crystalline compound **4** could be stored in air for 6 months.

Scheme 2. S_NAr Reaction of **3** with Phenyllithium

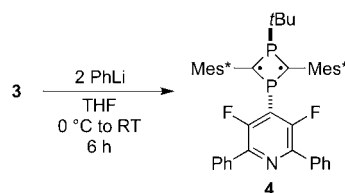


Table 1 compares the UV–vis data and the oxidation potentials of **3** and **4** with the highest occupied and lowest

Table 1. Physical Properties of the Pyridyl-Substituted Biradicals

product	λ_{\max}^a /nm	$\Delta E_{\text{HOMO-LUMO}}^b$ /eV	E_{pa}^c /V	E_{HOMO}^b /eV
3	608	4.76	0.61 0.84	−5.82
4	596	4.80	0.48 ^d	−5.68

^aVisible region in dichloromethane. ^bM06-2X/6-31G(d) level. ^cVolts vs Ag/AgCl. Conditions: 1 mM in dichloromethane, 0.1 M TBAP, working electrode GC, counter electrode Pt, scan rate 50 mV s^{−1}. ^d $E_{\text{pc}} = 0.39$ V.

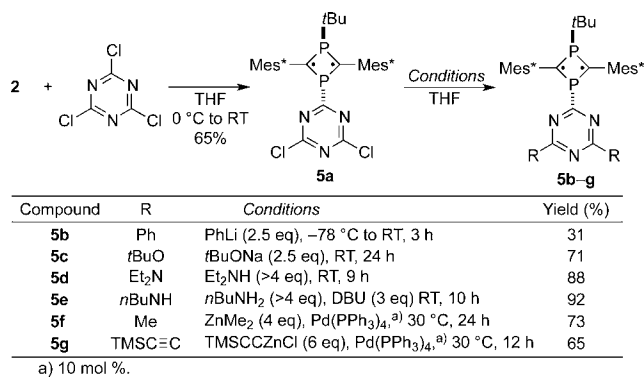
unoccupied molecular orbitals (HOMO and LUMO, respectively) of the DFT-optimized structures [M06-2X/6-31G(d) level].^{19,20} Compounds **3** and **4** showed a HOMO–LUMO transition absorption comparable to that of biradical **B**.^{10h} The perfluoropyridyl groups reduce the LUMO level [$E_{\text{LUMO}} = -1.06$ eV (**3**), -0.881 eV (**4**)], and the HOMO level was also affected by the σ -electron-withdrawing effect of fluorine. The presence of four electronegative fluorine atoms meant that **3**

displayed a higher, irreversible oxidation potential and an extra peak, probably from the decomposition product of the first oxidation. In contrast, **4** showed a lower oxidation potential because it contained fewer fluorine atoms, and the HOMO level seemed to be increased. Despite the electronegative substituents, **3** and **4** displayed irreversible reduction potentials around -0.80 V, probably because the P–aryl bond is unstable upon reduction.^{5c,11b,18} In the ^{19}F NMR spectrum, **4** showed a large J_{PF} constant (25.7 Hz), indicating the conjugation extended between the lone pair and the teraryl structure.

$\text{S}_{\text{N}}\text{Ar}$ Reaction for Triazine-Substituted 1,3-Diphosphacyclobutane-2,4-diyls. The $\text{S}_{\text{N}}\text{Ar}$ reaction of **2** with perfluorinated pyridine directly introduced the P-heterocycle and perfluoropyridyl groups, although the reaction was slow, and most postfunctionalization was not possible. Furthermore, the physicochemical properties of **3** and **4** indicated that the fluorinated pyridyl groups are restrictive. Therefore, we chose 2,4,6-trichloro-1,3,5-triazine (cyanuric chloride) as a reagent for direct arylation of **2**. Cyanuric chloride is used for the synthesis of a number of functionalized *s*-triazine derivatives,²¹ and we expected that the highly electron-deficient N-heteroaromatic structure would allow us to install the P-heterocyclic biradical moiety via nucleophilic aromatic substitution. Furthermore, postfunctionalization of the triazine skeleton by subsequent $\text{S}_{\text{N}}\text{Ar}$ reaction of the chlorine atoms should proceed smoothly.²²

Anion **2** was allowed to react with cyanuric chloride at 0 °C to room temperature in THF, and the desired $\text{S}_{\text{N}}\text{Ar}$ reaction took place to afford the corresponding triazine-substituted biradical **5a** in a moderate yield as a deep green solid (Scheme 3, step 1). Although crystalline **5a** could be handled in air, it

Scheme 3. $\text{S}_{\text{N}}\text{Ar}$ Reaction of **2** with 2,4,6-Trichloro-1,3,5-triazine



gradually decomposed under ambient conditions and requires storage under an inert atmosphere at -20 °C. The subsequent dual $\text{S}_{\text{N}}\text{Ar}$ reaction was also successful for the reactions of **5a** with phenyllithium, sodium *tert*-butoxide, diethylamine, and butylamine, and the corresponding P-heterocyclic biradicals **5b–e** were obtained in moderate to high yields (Scheme 3, step 2). The Negishi cross-coupling reaction²³ was used for the less thermally stable P-heterocyclic biradical **5a**, and the dimethyl- and bis(trimethylsilyl)ethynyl-substituted derivatives **5f** and **5g** were obtained in moderate yields (Scheme 3, step 2). Crystalline **5b–f** can be handled in air at room temperature, although they require storage under inert conditions. In contrast, Sonogashira coupling conditions were not suitable for preparing **5g** because of an undesirable Hoffmann reaction

with the amine. The ^{31}P NMR chemical shift of the *tert*-butyl-substituted phosphorus nuclei in **5** depended strongly on the substituents at the 3- and 5-positions of the 2,4,6-triazinyl group, and electron-withdrawing substituents induced lower ^{31}P chemical shifts. Furthermore, the $^2J_{\text{PP}}$ spin–spin coupling constants were reduced by electron-deficient substituents (see the Supporting Information). However, the phosphorus atoms on the triazine ring in **5** showed similar chemical shifts, probably because of the unique electronic properties of the singlet biradical bearing the skeletal *t*BuP structure.¹⁰ⁱ

Table 2 summarizes the UV–vis absorption properties, oxidation potentials, HOMO–LUMO energy differences, and

Table 2. Physical Properties of the Triazine-Substituted Biradicals

	$\lambda_{\text{max}}^{\text{a}}$ /nm	$\lambda_{\text{edge}}^{\text{a}}$ /eV	$\Delta E_{\text{HOMO-LUMO}}^{\text{b}}$ /eV	$E_{1/2}^{\text{oxc}}$ /V	$E_{\text{HOMO}}^{\text{b}}$ /eV
5a	692	1.18	4.38	0.50	-5.76
5b	659	1.33	4.45	0.35	-5.52
5c	630	1.43	4.52 ^d	0.31	-5.43^{d}
5d	627	1.44	4.54	0.18	-5.35
5f	643	1.33	4.51	0.34	-5.51
5g	674	1.28	4.37 ^e	0.40	-5.59^{e}

^aIn dichloromethane. ^bM06-2X/6-31G(d) level. ^cVolts vs Ag/AgCl. Conditions: 1 mM in dichloromethane, 0.1 M TBAP, working electrode GC, counter electrode Pt, scan rate 50 mV s⁻¹. Ferrocene/ferricinium +0.50 V. ^dInstead of *tert*-butoxy groups, methoxy groups were employed for DFT calculation. ^eInstead of (trimethylsilyl)ethynyl groups, ethynyl groups were employed for DFT calculation.

HOMO energies at the M06-2X/6-31G(d) level¹⁹ of **5**. The absorption maxima around 600–700 nm, assigned as a HOMO to LUMO transition, corresponded to the ΔE value between the HOMO and LUMO. Compared with **B**, the visible absorption of **5** showed a substantial red shift caused by the triazine, and the chlorine atom and ethynyl group reduced the HOMO–LUMO gap of the P-heterocyclic singlet biradical. The LUMO of **5a** in Figure 2a indicates a considerable

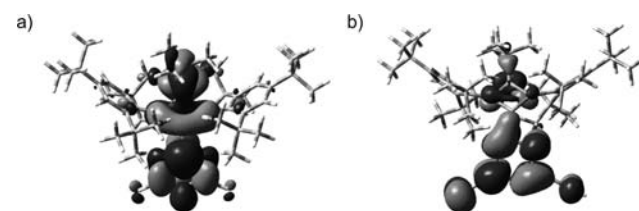


Figure 2. LUMOs of (a) **5a** and (b) **5g**.

contribution from the *s*-triazine moiety, and thus, the electron-deficient N-heteroaryl group reduces the band gap. However, in **5g** the ethynyl groups mainly contributed to the LUMO, and coefficients of the P-heterocyclic biradical skeleton are reduced in the LUMO (Figure 2b). Thus, the HOMO–LUMO transition of **5g** possesses charge-transfer excitation properties. In contrast, introducing π -electron-donating substituents, such as alkoxy and amino groups, effectively increased the HOMO–LUMO gap. The amino groups were particularly effective in maintaining the electron-donating properties of the P-heterocyclic biradical moiety; thus, the oxidation potential of **5d** was low.

Figures 3 and 4 show the structures of **5b** and **5d**, respectively. The metric parameters are summarized in Table S1 (Supporting Information). The structure of **5b** indicates that

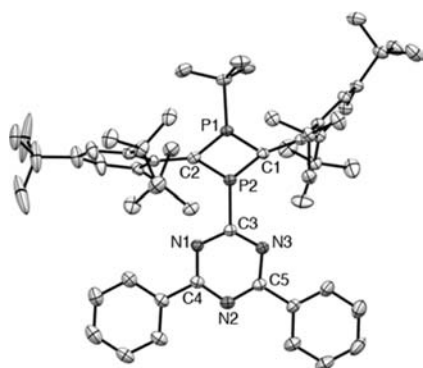


Figure 3. ORTEP drawing of the molecular structure of **5b** (40% probability levels). Hydrogen atoms and the solvent molecule (dichloromethane) are omitted for clarity. The 4-*C*(*t*Bu) group is disordered, and the atoms of higher occupancy factor (0.58) are shown.

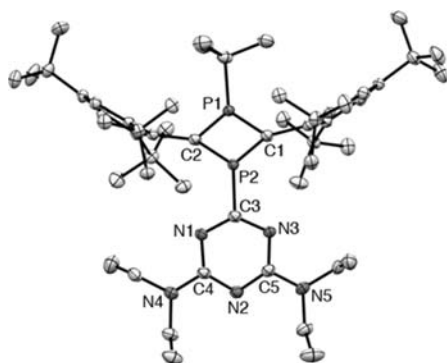


Figure 4. ORTEP drawing of the molecular structure of **5d** (50% probability levels). Hydrogen atoms are omitted for clarity. The phosphorus atoms are disordered, and the atoms of higher occupancy factor (0.96) are shown.

the phenyl rings with the adjacent triazine ring and the teraryl skeleton adopted a π -stacked dimeric structure (see Figure S1, Supporting Information). The nitrogen atoms in the diethylamino groups of **5d** are planar because of the conjugation between the lone pairs and the triazine π -system. These structural features around the triazine ring are consistent with the substituent effects. However, the sums of the bond angles around the P-aryl phosphino groups [317.54° (**5b**), 319.11° (**5d**)] indicate that the phosphorus atoms are considerably less hybridized and are very pyramidal. The lone pairs of the phosphorus atoms would still allow conjugation with the directly connected π -conjugate structure, because the PCPC ring skeleton would require enough electrons to stabilize the biradical system.²⁴ The crystal structure of **5e** contains H-bonds which form a dimeric structure (Figure S3, Supporting Information).

Semiconductor Properties of 1,3-Diphosphacyclobutane-2,4-diyl. The low oxidation potential of **5d** suggests facile electron release from the biradical chromophore would generate corresponding holes. In this study we focused on the field-effect transistor (FET) properties of **5d**. An FET device was fabricated by drop-casting a toluene solution of **5d** on a Si/SiO₂ wafer with interdigitated Au bottom electrodes. The silica dielectric surface was not treated. The measurements were conducted in situ, and Figure 5 shows the transfer plot. The **5d** FET device exhibited p-type semiconducting behavior with a

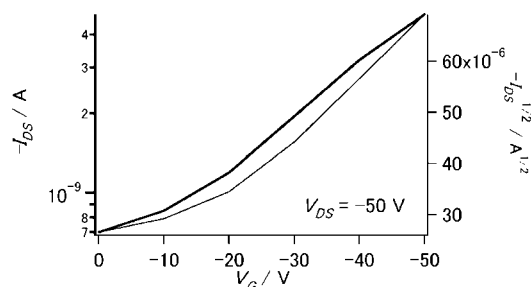


Figure 5. Transfer plots of an FET based on **5d** by using a bare silica dielectric surface.

relatively low threshold voltage of -6 V. However, the mobility of $2.3 \times 10^{-8} \text{ cm}^2 \text{ V}^{-1} \text{ s}^{-1}$ and the on/off ratio of 7 were too small for the material to be of practical use (Figure 5; Figure S4, Supporting Information). The crystal structure of **5d** indicates no obvious intermolecular π - π interaction (Figure S2, Supporting Information), which would explain the poor mobility and on/off ratio. Nevertheless, the facile electron release may allow semiconducting behavior. The ionization potential (IP) of crystalline **5d** (Figure 6) is as low as that of an evaporated thin film of air-stable dianthra[2,3-*b*:2',3'-*f*]thieno[3,2-*b*]thiophene (DATT), which is composed of eight fused π -aromatic rings (5.14 eV).²⁵

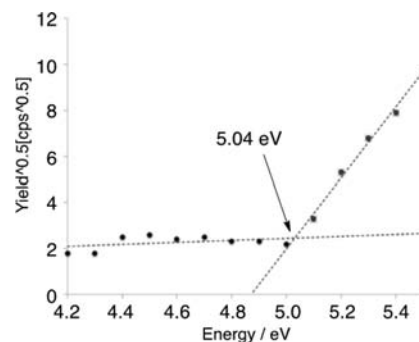


Figure 6. Photoelectron yield spectroscopy in air of crystalline **5d**.

The semiconducting character of **5d** is similar to that of **B** ($V_{\text{th}} = -0.1$ V, $\mu = 1.67 \times 10^{-7} \text{ cm}^2 \text{ V}^{-1} \text{ s}^{-1}$, on/off ratio 70; Figures S5 and S6, Supporting Information). The slightly superior properties of **B** compared with those of **5d** may arise from the nonsolvate crystal structure, which contains an offset intermolecular π - π interaction²⁶ (Figure S15, Supporting Information).

Preparation of a Tetraaryl-Substituted 1,3-Diphosphacyclobutane-2,4-diyl via SET Processes. In addition to nucleophilic substitution of the P-heterocyclic anion, the corresponding air-tolerant crystalline 1,3-diphosphacyclobuten-4-yl radicals²⁷ can be accessed through a one-electron oxidation. We speculated that coupling the P-heterocyclic monoradical with other radical species would be an effective method for constructing P-heterocyclic biradicals.

Phosphaalkyne **1** was allowed to react with 1 equiv of phenyllithium in THF to generate the corresponding cyclobutenyl anion **2'**. The formation of **2'** [δ_{p} (THF/C₆D₆) 275.7, 50.0 ppm; $^2J_{\text{PP}} = 89.5$ Hz] indicates that the intermediate phosphavinyl anion promptly reacted with **1**. The mixture of **2'** and phenyllithium was subsequently treated with iodine at room temperature to generate monoradical **6** and the phenyl

radical. After removal of volatile materials and washing with acetonitrile, novel biradical **7** was obtained as a deep-blue solid in a moderate yield (Scheme 4). Crystalline biradical **7** showed extremely high stability in air, and the structure was not altered after exposure to air for 1 year.

Scheme 4. SET-Based Preparation of **7** from **1** through Intermediates **2'** and **6**

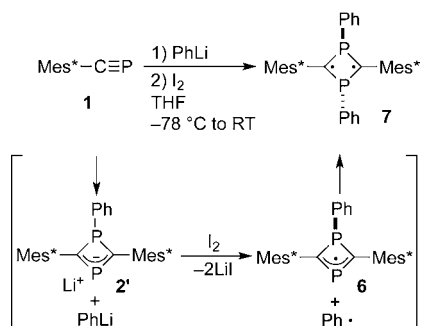


Figure 7 shows an ORTEP drawing for **7** determined by conventional crystallographic analysis. The molecular structure

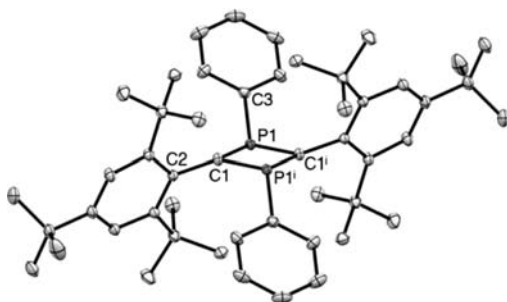


Figure 7. ORTEP drawing for the X-ray structure of **7** (50% probability levels). Hydrogen atoms are omitted for clarity. Selected bond lengths (Å) and angles (deg): P1–C1, 1.7463(2); P1ⁱ–C1, 1.7502(2); C1–C2, 1.4883(3); P1–C3, 1.8055(3); C1–P1–C1ⁱ, 93.12(2); C1–P1–C3, 121.88(1); C3–P1–C1ⁱ, 117.78(1); P1–C1–P1ⁱ, 86.88(1); P1–C1–C2, 139.55(2); P1ⁱ–C1–C2, 129.54(2) (superscript “i” indicates symmetry code 1 – x, 1 – y, 1 – z).

possesses a symmetric point, and the two [Mes*CPPh] moieties are equivalent. The skeletal P–C lengths of **7** are equivalent, and the rhomboidal four-membered ring showed high planarity ($\tau = 0.0^\circ$). The phosphino groups exhibited an sp^3 -like structure, and the skeletal carbon atoms were sp^2 hybridized (sum of bond angles: P, 332.5° ; C1, 356.1°). The dihedral angle between the Mes* aromatic ring and the biradical skeleton of $\tau = 69.1^\circ$ indicates a small contribution from the conjugation effect. The $C_{\text{ipso}}-C_{\text{ortho}}$ and $C_{\text{ortho}}-t\text{Bu}$ lengths in the Mes* moiety indicate a distortion corresponding to a boat conformation,²⁸ probably arising from the steric hindrance. The X-ray structure of **7** is almost identical to the DFT-calculated structure [M06-2X/6-31G(d)].¹⁹

A drop-cast device composed of **7** displayed no FET response. The electron-donating properties of **7** are slightly less than those of **5d** and **B** because the phosphorus atoms are directly bound to electron-withdrawing phenyl groups. In the crystal structure, no interaction between the aryl substituents was observed, whereas the centroid–centroid distance between the four-membered rings of 8.701 Å is shorter than that of **B**.

However, the direct P–aryl linkage would not necessarily be a disadvantage for suitable molecular and crystal structures of P-heterocyclic biradicals with semiconducting properties, and P-heterocyclic biradicals may still be promising candidates for organic field-effect transistors, offering some structural improvements and better device fabrication.

Electron Density Distribution of the Symmetrical 1,3-Diphosphacyclobutane-2,4-diyl. Single-crystal X-ray diffraction data of **7** were obtained to analyze the electron density distribution in detail. The diffraction data were measured up to $[(\sin \theta)/\lambda]_{\text{max}} = 1.22 \text{ \AA}^{-1}$ using Mo $K\alpha$ radiation at 90 K (see the Supporting Information). A 3D plot of the static model density of **7** (Figure 8; Figure S10,

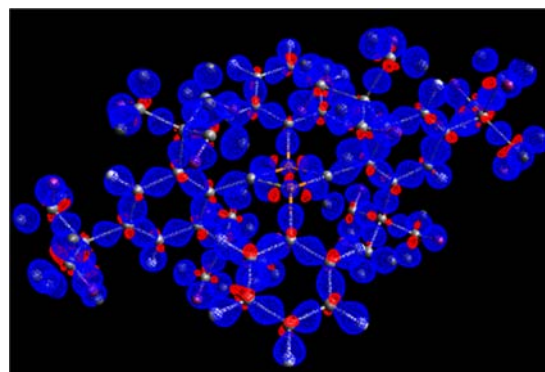


Figure 8. Three-dimensional view plot of **7** displaying electron-increased (blue) and electron-decreased (red) areas by construction of the molecule.

Supporting Information) indicates that all the covalent bonds except for those in the four-membered ring were conventional σ - and π -bonds. Figure 9 shows static model density maps of **7** on the PCPC plane (top) and the cross section of the PCPC plane through the skeletal carbons (bottom). The bent skeletal P–C bonds are clearly visible in the map on the PCPC plane.

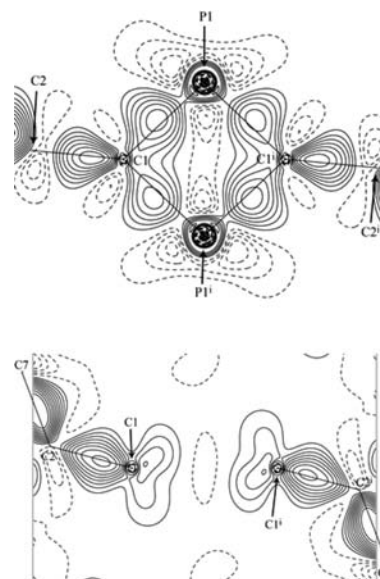


Figure 9. Static model maps of **7** on the PCPC plane (top) and the cross section of the PCPC plane through the skeletal carbons (bottom). Solid and broken lines indicate positive and negative densities, respectively. The contours are drawn at a 0.05 e \AA^{-3} interval.

The map also shows high endocyclic electron density around the skeletal carbons. The p-like shape of the radical electron orbitals was characterized by the plane perpendicular to the PCPC plane. The p-like structure of the vertically unsymmetrical distribution at the rims of skeletal carbons was unusually distorted. The distortion may be caused by the small influence of the sp^3 -hybridization. The pyramidalized phosphorus atoms indicate a structure similar to that of usual trisubstituted phosphines and the delocalization of the lone pairs in both the s - and sp^3 -shaped orbitals.

Figure 10 shows the experimentally determined bond paths, bond critical points (BCPs), and a ring critical point (RCP) for

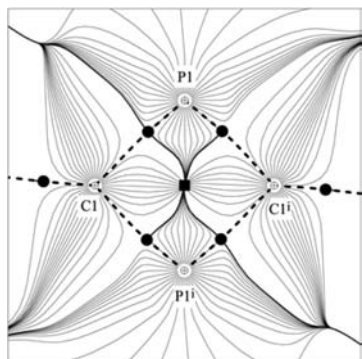


Figure 10. Gradient trajectories (fine lines), bond paths (broken lines), bond critical points (BCPs; circles), and ring critical point (RCP; square) in the four-membered heterocycle plane of **7**. Bond ellipticity at the BCPs: P(1)–C(1), 0.37; P(1)–C(1)ⁱ, 0.57; C(1)–C_{Mes*}, 0.03.

the four-membered cycle of **7**. The RCP indicates there were no bonding interactions between the transannular C...C and P...P areas. Slightly bent bond paths were observed in the four-membered ring, which are common in small rings. The bond ellipticity of the skeletal P–C bonds was created by a large accumulation of electron density at the skeletal carbon atoms by the adjacent electropositive phosphorus atoms and the covalent bonds. Hence, the P–C linkages in the four-membered ring²⁹ were distinct from those of acyclic phosphorus ylides.³⁰ The electron density map and the BCP data for **7** indicate the contribution of the two canonical forms which describe 1,3-diphosphacyclobutane-2,4-diyl on the basis of the difference between carbon and phosphorus. Additionally, Figure S11 (Supporting Information) shows a Laplacian distribution plot on the PCPC plane. The low bond ellipticity of the bond between the skeletal carbon and Mes* group may indicate a trace conjugative interaction between the four-membered ring and the aryl ring. Therefore, the π -overlap between the PCPC ring and the Mes* aryl plane is small, and the π -delocalization between the PCPC ring and Mes* aryl skeleton is negligible. The extreme stability probably depends on the steric hindrance around the radical centers. The experimentally determined bond characteristics of **7**, including BCPs and RCPs, were also determined by the AIM calculations based on the DFT data (Figure S12, Supporting Information). These electron density distribution characteristics were also confirmed by studies of **B** (see the Supporting Information).

CONCLUSION

We synthesized N-heteroaryl-substituted 1,3-diphosphacyclobutane-2,4-diyls **3** and **5a** by S_NAr reactions of the thermally

stable 1,3-diphosphacyclobuten-4-yl anion **2** with electron-deficient N-heteroaromatic reagents. We subsequently used S_NAr and the Negishi cross-coupling reactions to obtain **4** and **5b–g**. The direct link between the P-heterocyclic biradical skeleton and N-heteroaromatic structure enabled effective tuning of the MOs to vary the physicochemical properties of the stable P-heterocyclic biradical moiety via the considerable conjugative interaction. The six-membered conjugative N-heterocyclic structures were highly electronegative, and the amino-substituted triazine produced a strongly electron-donating biradical unit that exhibited unique p-type semiconductor behavior. The SET reaction afforded tetraaryl-substituted 1,3-diphosphacyclobutane-2,4-diyl **7** as a highly air-stable crystalline compound, indicating that the radical-induced method is a practical approach for accessing various P-heterocyclic biradicals. Single-crystal X-ray diffraction of **7** revealed unusual electron density distributions, including very localized radicalic electrons. Precise structural analyses would explain the unique physicochemical properties and also allow further studies of singlet open-shell molecular entities. This study has demonstrated the utility of the P-aryl moiety for tuning the electronic and structural properties of the P-heterocyclic biradical system. We are currently developing functional and practical organic materials based on this work.

ASSOCIATED CONTENT

Supporting Information

Experimental details for preparation of **3–5** and **7**, physicochemical data of **3–5** and **7**, X-ray crystallographic data of **5b**, **5d**, **5e**, **7**, and nonsolvate **B**, DFT and AIM calculation data of **5**, **7**, and **B**, copies of NMR charts, and CIF data. This material is available free of charge via the Internet at <http://pubs.acs.org>.

AUTHOR INFORMATION

Corresponding Author

ito.s.ao@m.titech.ac.jp

Notes

The authors declare no competing financial interest.

ACKNOWLEDGMENTS

This work was supported in part by Grants-in-Aid for Scientific Research (Nos. 22350058 and 23655173 for S.I. and No. 25109543 for D.H.) from the Ministry of Education, Culture, Sports, Science and Technology, Japan, and Nissan Chemicals Co. Ltd. for S.I. We thank Prof. Dr. Hiroharu Suzuki and Dr. Masataka Oishi of the Tokyo Institute of Technology for support of X-ray crystallographic analyses and Dr. Yoshiyuki Nakajima of Riken Keiki Co., Ltd. for measurements of photoelectron yield spectroscopy in air. UV–vis spectroscopic measurements were supported by Prof. Yuji Wada and Dr. Masato Maitani of the Tokyo Institute of Technology.

REFERENCES

- (1) (a) Hicks, R. G., Ed. *Stable Radicals—Fundamentals and Applied Aspects of Odd-Electron Compounds*; Wiley: Chichester, U.K., 2010. (b) Martin, C. D.; Soleilhavoup, M.; Bertrand, G. *Chem. Sci.* **2013**, *4*, 3020–3030.
- (2) (a) Jain, R.; Sponsler, M. B.; Coms, F. D.; Dougherty, D. A. *J. Am. Chem. Soc.* **1988**, *110*, 1356–1366. (b) Bush, L. C.; Heath, R. B.; Berson, J. A. *J. Am. Chem. Soc.* **1993**, *115*, 9830–9831.
- (3) (a) Berson, J. A. *Acc. Chem. Res.* **1997**, *30*, 238–244. (b) Dougherty, D. A. *Acc. Chem. Res.* **1991**, *24*, 88–84.

- (4) (a) Niecke, E.; Fuchs, A.; Baumeister, F.; Nieger, M.; Schoeller, W. W. *Angew. Chem., Int. Ed. Engl.* **1995**, *34*, 555–557. (b) Schoeller, W. W.; Begemann, C.; Niecke, E.; Gudat, D. *J. Phys. Chem. A* **2001**, *105*, 10731–10738.
- (5) (a) Schmidt, O.; Fuchs, A.; Gudat, D.; Nieger, M.; Hoffbauer, W.; Niecke, E.; Schoeller, W. W. *Angew. Chem., Int. Ed.* **1998**, *37*, 949–952. (b) Niecke, E.; Fuchs, A.; Nieger, M. *Angew. Chem., Int. Ed.* **1999**, *38*, 3028–3031. (c) Niecke, E.; Fuchs, A.; Nieger, M.; Schmidt, O.; Schoeller, W. W. *Angew. Chem., Int. Ed.* **1999**, *38*, 3031–3034. (d) Sebastian, M.; Schmidt, O.; Fuchs, A.; Nieger, M.; Szieberth, D.; Nyulászi, L.; Niecke, E. *Phosphorus, Sulfur Silicon Relat. Elem.* **2004**, *179*, 779–783. (e) Sebastian, M.; Nieger, M.; Szieberth, D.; Nyulászi, L.; Niecke, E. *Angew. Chem., Int. Ed.* **2004**, *43*, 637–641. (f) Sebastian, M.; Hoskin, A.; Nieger, M.; Nyulászi, L.; Niecke, E. *Angew. Chem., Int. Ed.* **2005**, *44*, 1405–1408. (g) Fuchs, A.; Gudat, D.; Nieger, M.; Schmidt, O.; Sebastian, M.; Nyulászi, L.; Niecke, E. *Chem.—Eur. J.* **2002**, *8*, 2188–2196.
- (6) Perstanna[1.1.1]propellanes: Sita, L. R.; Kinoshita, I. *J. Am. Chem. Soc.* **1992**, *114*, 7024–7029.
- (7) Heavier congeners of cyclobutane-1,3-diyl: (a) Scheschke, D.; Amii, H.; Gornitzka, H.; Schoeller, W. W.; Bourissou, D.; Bertrand, G. *Science* **2002**, *295*, 1880–1811. (b) Cui, C.; Brynda, M.; Olmstead, M. M.; Power, P. P. *J. Am. Chem. Soc.* **2004**, *126*, 6510–6511. (c) Cox, H.; Hitchcock, P. B.; Lappert, M. F.; Pierrsens, L. J.-M. *Angew. Chem., Int. Ed.* **2004**, *43*, 4500–4504. (d) Dickie, D. A.; Lee, P. T. K.; Labeodan, O. A.; Schatte, G.; Weinberg, N.; Lewis, A. R.; Bernard, G. M.; Wasylshen, R. E.; Clyburne, J. A. C. *Dalton Trans.* **2007**, 2862–2869. (e) Wang, X.; Peng, Y.; Olmstead, M. M.; Fetting, J. C.; Power, P. P. *J. Am. Chem. Soc.* **2009**, *131*, 14164–14165. (f) Henke, P.; Pankewitz, T.; Klopfer, W.; Breher, F.; Schnöckel, H. *Angew. Chem., Int. Ed.* **2009**, *48*, 8141–8145. (g) Beweries, T.; Kuzora, R.; Rosenthal, U.; Schulz, A.; Villinger, A. *Angew. Chem., Int. Ed.* **2011**, *50*, 8974–8978. (h) Takeuchi, K.; Ichinohe, M.; Sekiguchi, A. *J. Am. Chem. Soc.* **2011**, *133*, 12478–12481. (i) Demeshko, S.; Godemann, C.; Kuzora, R.; Schulz, A.; Villinger, A. *Angew. Chem., Int. Ed.* **2013**, *52*, 2105–2108. See also: (j) Dodd, A.; Gemel, C.; Winter, M.; Fischer, R. A.; Goedecke, C.; Rzepa, H. S.; Frenking, G. *Angew. Chem., Int. Ed.* **2013**, *52*, 450–454. (k) Mondal, K. C.; Roesky, H.; Schwarzer, M. C.; Frenking, G.; Tkach, I.; Wolf, H.; Kratzert, D.; Herbst-Irmer, R.; Niepötter, B.; Stalke, D. *Angew. Chem., Int. Ed.* **2013**, *52*, 1801–1805. (l) Singh, A. P.; Samuel, P. P.; Roesky, H. W.; Schwarzer, M. C.; Frenking, G.; Sidhu, N. S.; Ditttrich, B. *J. Am. Chem. Soc.* **2013**, *135*, 7324–7329. (m) Katagiri, T.; Sakai, T.; Mizuta, T.; Fujiwara, Y.; Abe, M. *Chem.—Eur. J.* **2013**, *19*, 10395–10404.
- (8) (a) Breher, F. *Coord. Chem. Rev.* **2007**, *251*, 1007–1043. (b) Grützmacher, H.; Breher, F. *Angew. Chem., Int. Ed.* **2002**, *41*, 4006–4011. (c) Abe, M. *Chem. Rev.* **2013**, *113*, 7011–7088. (d) Power, P. P. *Chem. Rev.* **2003**, *103*, 789–809.
- (9) Sugiyama, H.; Ito, S.; Yoshifuji, M. *Angew. Chem., Int. Ed.* **2003**, *42*, 3802–3804.
- (10) (a) Sugiyama, H.; Ito, S.; Yoshifuji, M. *Chem.—Eur. J.* **2004**, *10*, 2700–2706. (b) Yoshifuji, M.; Sugiyama, H.; Ito, S. *J. Organomet. Chem.* **2005**, *690*, 2515–2520. (c) Ito, S.; Kikuchi, M.; Sugiyama, H.; Yoshifuji, M. *J. Organomet. Chem.* **2007**, *692*, 2761–2767. (d) Ito, S.; Miura, J.; Morita, N.; Yoshifuji, M.; Arduengo, A. J., III. *Angew. Chem., Int. Ed.* **2008**, *47*, 6418–6421. (e) Ito, S.; Miura, J.; Morita, N.; Yoshifuji, M.; Arduengo, A. J., III. *Z. Anorg. Allg. Chem.* **2009**, *635*, 488–495. (f) Ito, S.; Miura, J.; Morita, N.; Yoshifuji, M.; Arduengo, A. J., III. *Heteroat. Chem.* **2010**, *21*, 404–411. (g) Ito, S.; Miura, J.; Morita, N.; Yoshifuji, M.; Arduengo, A. J., III. *C. R. Chim.* **2010**, *13*, 1180–1184. (h) Ito, S.; Kikuchi, M.; Miura, J.; Morita, N.; Yoshifuji, M. *J. Phys. Org. Chem.* **2012**, *25*, 733–737. (i) Yoshifuji, M.; Osborn, S. T.; Arduengo, A. J., III; Belmore, K. B.; Ito, S. *Heteroat. Chem.* **2011**, *22*, 331–338. (j) Yoshifuji, M.; Hirano, Y.; Schnakenburg, G.; Streubel, R.; Niecke, E.; Ito, S. *Helv. Chim. Acta* **2013**, *95*, 1723–1729.
- (11) (a) Ito, S.; Miura, J.; Morita, N.; Yoshifuji, M.; Arduengo, A. J., III. *Inorg. Chem.* **2009**, *48*, 8063–8065. (b) Ito, S.; Miura, J.; Morita, N.; Yoshifuji, M.; Arduengo, A. J., III. *Dalton Trans.* **2010**, *39*, 8281–8287.
- (12) Ito, S.; Kobayashi, M.; Mikami, K. *Org. Lett.* **2013**, *15*, 3404–3407.
- (13) Nyulászi, L. *Chem. Rev.* **2001**, *101*, 1229–1246.
- (14) Schoeller, W. W.; Niecke, E. *Phys. Chem. Chem. Phys.* **2012**, *14*, 2015–2023.
- (15) Ye, J.; Fujiwara, Y.; Abe, M. *Beilstein J. Org. Chem.* **2013**, *9*, 925–933.
- (16) Study of isomers of hexasilabenzene: Kratzert, D.; Leussler, D.; Holstein, J. J.; Ditttrich, B.; Abersfelder, K.; Scheschke, D.; Stalke, D. *Angew. Chem., Int. Ed.* **2013**, *52*, 4478–4482.
- (17) (a) Bellabarba, R. M.; Nieuwenhuyzen, M.; Saunders, G. C. *Organometallics* **2003**, *22*, 1802–1810. (b) Goryunov, L. I.; Grobe, J.; Shteingarts, V. J.; Krebs, B.; Lindemann, A.; Würthwein, E.-U.; Mück-Lichtendfeld, C. *Chem.—Eur. J.* **2000**, *6*, 4612–4622. (c) Goryunov, L. I.; Shteingarts, V. D.; Grobe, J.; Krebs, B.; Triller, M. U. *Z. Anorg. Allg. Chem.* **2002**, *628*, 1770–1779.
- (18) Ito, S.; Ngo, T. T. T.; Mikami, K. *Chem.—Asian J.* **2013**, *8*, 1976–1980.
- (19) Zhao, Y.; Truhler, D. G. *Theor. Chem. Acc.* **2008**, *120*, 215–241.
- (20) Although 1,3-diphosphacyclobutane-2,4-diyls exhibit open-shell properties to some extent, the terms “HOMO” and “LUMO” are used formally to describe higher and lower energetic molecular orbitals.
- (21) Hoge, B.; Wiebe, W. *Angew. Chem., Int. Ed.* **2008**, *47*, 8116–8119.
- (22) (a) Hayashi, M.; Yamasaki, T.; Kobayashi, Y.; Imai, Y.; Watanabe, Y. *Eur. J. Org. Chem.* **2009**, 4956–4962. (b) Blotny, G. *Tetrahedron* **2006**, *62*, 9507–9522. (c) Steffensen, M. B.; Hollink, E.; Kuschel, F.; Bauer, M.; Simanek, E. E. *J. Polym. Sci., Part A: Polym. Chem.* **2006**, *44*, 3411–3433. (d) Gamez, P.; Reedijk, J. *Eur. J. Inorg. Chem.* **2006**, 29–42.
- (23) (a) Negishi, E.-i.; Baba, S. *J. Chem. Soc., Chem. Commun.* **1976**, 596–597. (b) King, A. O.; Negishi, E.-i. *J. Chem. Soc., Chem. Commun.* **1977**, 683–684.
- (24) The stability of the biradical skeleton was dramatically reduced by replacing the *tert*-butyl group with primary alkyl groups. See ref 18.
- (25) Niimi, K.; Shinamura, S.; Osaka, I.; Miyazaki, E.; Takimiya, K. *J. Am. Chem. Soc.* **2011**, *133*, 8732–8739.
- (26) Janiak, C. *J. Chem. Soc., Dalton Trans.* **2000**, 3885–3896.
- (27) Ito, S.; Kikuchi, M.; Morita, N.; Yoshifuji, M.; Arduengo, A. J., III; Konovalova, T. A.; Kispert, L. D. *Angew. Chem., Int. Ed.* **2006**, *45*, 4341–4345.
- (28) (a) Yoshifuji, M.; Shima, I.; Inamoto, N.; Aoyama, T. *Tetrahedron Lett.* **1981**, *22*, 3057–3060. (b) Yoshifuji, M.; Shima, I.; Inamoto, N.; Hirotsu, K.; Higuchi, T. *Angew. Chem., Int. Ed. Engl.* **1980**, *19*, 399–400. (c) Yoshifuji, M.; Inamoto, N.; Hirotsu, K.; Higuchi, T. *J. Chem. Soc., Chem. Commun.* **1985**, 1109–1111. (d) Ito, S.; Miyake, H.; Yoshifuji, M. *ARKIVOC* **2012**, part ii, 6–14.
- (29) Absar, I.; Schaad, L. J.; Van Waser, J. R. *Theor. Chim. Acta* **1973**, *29*, 173–181.
- (30) Yufit, D. S.; Howard, J. A. K.; Davidson, M. D. *J. Chem. Soc., Perkin Trans. 2* **2000**, 249–253.